Experimental Animals
Exp. Anim. 71(3), 305–315, 2022

Original

MicroRNA-363-3p/sphingosine-1-phosphate receptor 1 axis inhibits sepsis-induced acute lung injury via the inactivation of nuclear factor kappa-B ligand signaling

Shishuai MENG[1)], Kai KANG[1)], Dongsheng FEI[1)], Songlin YANG[1)], Shangha PAN[2)], Kaijiang YU[2,3)] and Mingyan ZHAO[1)]

[1)]*Department of Intensive Care Unit, The First Affiliated Hospital of Harbin Medical University, No. 23 Youzheng Street, Harbin, Heilongjiang, 150001, P.R. China*
[2)]*Key Laboratory of Hepatosplenic Surgery, Ministry of Education, The First Affiliated Hospital of Harbin Medical University, No. 23 Youzheng Street, Harbin, Heilongjiang, 150001, P.R. China*
[3)]*The Cell Transplantation Key Laboratory of National Health Commission, No. 23 Youzheng Street, Harbin, Heilongjiang, 150001, P.R. China*

Abstract: Infection-associated inflammation and coagulation are critical pathologies in sepsis-induced acute lung injury (ALI). This study aimed to investigate the effects of microRNA-363-3p (miR-363-3p) on sepsis-induced ALI and explore the underlying mechanisms. A cecal ligation and puncture-induced septic mouse model was established. The results of this study suggested that miR-363-3p was highly expressed in lung tissues of septic mice. Knockdown of miR-363-3p attenuated sepsis-induced histopathological damage, the inflammation response and oxidative stress in lung tissues. Furthermore, knockdown of miR-363-3p reduced the formation of platelet-derived microparticles and thrombin generation in blood samples of septic mice. Downregulation of miR-363-3p suppressed sphingosine-1-phosphate receptor 1 (S1PR1) expression in lung tissues and subsequently inactivated the nuclear factor kappa-B ligand (NF-κB) signaling. A luciferase reporter assay confirmed that miR-363-3p directly targeted the 3'-untranslated region of the mouse *S1pr1* mRNA. Collectively, our study suggests that inactivation of NF-κB signaling is involved in the miR-363-3p/S1PR1 axis-mediated protective effect on septic ALI.
Key words: acute lung injury, inflammation, microRNA-363-3p (miR-363-3p)/sphingosine-1-phosphate receptor 1 (S1PR1) axis, nuclear factor kappa-B ligand (NF-κB) signaling, sepsis

Introduction

Sepsis is a clinical syndrome defined as a systemic inflammation in response to infection, which often causes life-threatening multiple organ dysfunction [1]. The lung is the organ most susceptible to sepsis, and more than 50% of patients with sepsis develop acute lung injury (ALI) [2]. During sepsis, disseminated intravascular coagulation and microvascular thrombosis aggravate clinical outcomes in patients with abdominal sepsis and eventually leads to a rise in mortality [3]. Despite the development of clinical practices for the treatment of abdominal sepsis, septic patients continue to have high mortality rate and poor prognosis [4]. It is necessary to understand the precise mechanisms of sepsis-induced ALI to improve survival in patients.

MicroRNAs (miRs) are small and conserved non-coding RNAs that negatively modulate gene expression by targeting the specific 3'-untranslated region (UTR) of messenger RNAs (mRNAs) [5]. As an abnormal expression of miRNAs is always observed in sepsis-induced ALI, subsets of miRNAs have been determined to be crucial regulators or biomarkers of septic ALI [6]. Furthermore, sepsis-induced coagulation dysfunction is cor-

(Received 17 September 2021 / Accepted 5 January 2022 / Published online in J-STAGE 16 February 2022)
Corresponding author: M. Zhao. email: 201701159@hrbmu.edu.cn.

related with some miRNAs [7, 8]. High expression of serum miR-122 aggravates coagulation disorder in sepsis patients [8]. MiR-126 overexpression inhibits septic inflammation and the thrombin-induced the increase of permeability via the AKT/Rac1 signaling pathway, thereby ameliorating the prognosis of septic mice [9]. Recent evidence reveals that downregulation of miR-363-3p ameliorates propofol-induced neurotoxicity via the inhibition of oxidative stress and apoptosis [10], implying potential negative effects of miR-363-3p. However, the functional and molecular mechanisms of miR-363-3p in sepsis-induced ALI remain poorly understood.

Sphingosine-1-phosphate (S1P) is produced via phosphorylation of sphingosine by an enzyme family consisting of two isoenzymes, which are named sphingosine kinase (SPHK) 1 and 2 [11]. The SPHK/S1P/S1P-receptor (S1PR) signaling axis in macrophages has been reported to be involved in the pathogenesis of inflammatory diseases, such as atherosclerosis, asthma, rheumatoid arthritis, and cancer [12]. As a downstream molecule bound with S1P, S1PR1 triggers a series of responses, including cell proliferation, migration, apoptosis and angiogenesis [13, 14]. A study has shown that macrophage S1PR1 deletion aggravates early inflammation in a mouse model of imiquimod-induced psoriasis [15]. The selective S1PR1 agonist CYM5442 protects against pulmonary injury induced by the 2009 influenza A H1N1 virus [16]. It has been proposed by Feng *et al*. that S1P and its receptor S1PR1 are potential therapeutic targets and biomarkers for sepsis [17]. Apolipoprotein M alleviates lipopolysaccharide (LPS)-induced ALI through the activation of S1P/S1PR1 signaling [18]. However, the effects of S1PR1 on sepsis are still unknown. A previous study suggests that there is a binding site of miR-363-3p within the 3'-UTR of human S1PR1 mRNA [19]. It has also been reported that miR-363-3p upregulation decreases the SPHK2 level in colorectal cancer cells [20]. Considering the above findings, we speculate that the miR-363-3p/S1PR1 axis may exert a crucial role in sepsis-induced ALI.

The current study aimed to elucidate the functional mechanisms of the miR-363-3p/S1PR1 axis in cecal ligation and puncture (CLP)-induced septic mice.

Materials and Methods

CLP-induced murine sepsis model

Male 8-week-old C57BL/6 mice were purchased from ChangSheng Biotech (Benxi, China). All the procedures in animal experiments followed the Guide for the Care and Use of Laboratory Animals, and this study was approved by the First Affiliated Hospital of Harbin Medical University (approval ID: YJSKYCX2018-46HYD). Mice were maintained under standard conditions (22 ± 1°C, 45–55% humidity, and 12-h day-night cycle) and had food and water available ad libitum. Following adaption, all mice were randomly assigned to i) a sham group, ii) a CLP group, iii) a CLP+antagomir NC group, and iv) a CLP+antagomir-363-3p group. The CLP procedure was performed to induce midgrade sepsis as previously described [21]. Under anesthesia with 50 mg/kg pentobarbital sodium, a 1 cm incision was made in the middle of the abdomen of the mice to expose the cecum. A 4-0 braided silk suture was passed through the midpoint between the colon root and cecum terminal to ligate the cecum. The ligated cecum was then punctured twice with a 21-gauge needle. Finally, the cecum was repositioned, and the incision was closed. Sham mice underwent the same surgical procedures except for the CLP.

MiR-363-3p antagomir injection

MiR-363-3p antagomir (antagomir-363-3p) and its negative control (NC) were synthesized and bought from GenePharma (Shanghai, China). Mice received tail vein intravenous injections of antagomir-363-3p or its NC at a dose of 60 μg/g body weight, as described in previous studies but with slight modification [22–24], 24 h before the CLP procedure. The sham and CLP groups only obtained equal volume of normal saline.

Survival analysis

Mice were monitored for survival status daily for 7 days after the CLP procedure. Except for those used for the survival analysis, mice were euthanized using 150 mg/kg pentobarbital sodium 24 h after the CLP procedure. The lung tissues and blood samples were harvested for subsequent experiments.

Hematoxylin and eosin (H&E) staining

Lung tissues of each mouse were fixed, dehydrated, embedded in paraffin, sliced into 5-μm sections, and deparaffinized. The sections were then stained with H&E for histological analysis. Representative histological images were acquired under BX53 light microscopy (Olympus, Tokyo, Japan) at 200× magnification. The degree of lung injury was determined using a semi-quantitative scoring system as described previously [21].

Pulmonary edema assessment

Pulmonary edema was evaluated by lung wet/dry weight ratio (W/D ratio) according to a previous study [21]. The lung tissues of each mouse were weighed and then dried at 65°C to obtain the W/D ratio: (wet weight/dry weight) ×100%.

Oxidative stress analysis

The lung tissues were homogenized in normal saline (weight:volume=1:9). The levels of oxidative stress-related markers, including reactive oxygen species (ROS), malondialdehyde (MDA), superoxide dismutase (SOD), and reduced glutathione (GSH), were detected in the tissue homogenates with the commercial kits (Jiancheng Bioengineering Institute, Nanjing, China) in accordance with the correspondingly manufacturer's instructions.

Bronchoalveolar lavage and isolation

Bronchoalveolar lavage fluid (BALF) was collected 24 h after the CLP procedure as previously reported [25]. A total of 1.5 ml phosphate buffer solution (PBS) was injected into the lungs via the trachea to obtain BALF. Total cells, macrophages, and neutrophils were counted in BALF using a hemacytometer. The cells were then stained with Wright-Giemsa (D010, Jiancheng Bioengineering Institute) and observed at ×200 magnification.

ELISA assay

The levels of myeloperoxidase (MPO), interleukin-1β (IL-1β), and tumor necrosis factor-α (TNF-α) in the lung tissue homogenates were detected by using commercial ELISA kits according to the manufacturer's instructions (Multiscience (Lianke) Biotech, Hangzhou, China).

Platelet-derived microparticles (PMPs) formation

Blood samples were lysed using RBC lysis buffer (420301, BioLegend, San Diego, CA, USA) and centrifuged at 350 g for 5 min. The pellets were resuspended in PBS buffer. Subsequently, 10^6 cells were incubated with the PE-anti-mouse CD41 antibody (133905, BioLegend) at 4°C for 20 min in the dark. PMP production was monitored using flow cytometry (NovoCyte) and analyzed by NovoExpress 1.2.5 (ACEA Biosciences, Inc., San Diego, CA, USA).

Thrombin generation (TG) assay

Thrombin activity was detected in blood samples using a Thrombin Activity Fluorometric Assay Kit (K373, Biovision, Milpitas, CA, USA) as recommended by the manufacturer.

Real-time polymerase chain reaction (RT-PCR)

Lung tissues were homogenized and total RNAs were isolated using TRIpure reagent (RP1201, BioTeke Corp., Beijing, China). Total RNA was reverse transcribed to cDNA using M-MLV Transcriptase (BioTeke Corp.). Subsequently, RT-PCR amplification was performed using a SYBR Green PCR Kit (Solarbio, Beijing, China). The primers used for PCR were as follows:, 5'-AATTGCACGGTATCCATCTGTA-3' (forward) and 5'-GTGCAGGGTCCGAGGT-3' (reverse) for miR-363-3p and 5'-CGCAAGAACATCTCCAAG-3' (forward) and 5'-CAGCACAGCCAGAACCAG-3' (reverse) for S1PR1. Relative mRNA expression was determined with the $2^{-\Delta\Delta CT}$ method [26] and normalized to β-actin or U6.

Western blotting

Lung tissues were homogenized and protein was isolated using the RIPA lysis solution (P0013B, Beyotime, Shanghai, China). Protein concentration was determined with a Bradford protein assay kit (P0009, Beyotime). A total of 15–30 μg protein per lane was separated on 10% SDS polyacrylamide gel and transferred onto a polyvinylidene fluoride membrane (Thermo Fisher Scientific, Waltham, MA, USA). Following blocking in TBST (TBS with 0.1% Tween-20) for 1 h, the membrane was incubated with anti-S1PR1 (1:500; A12935, ABclonal, Wuhan, China), anti-nuclear factor kappa-B (NF-κB) ligand p65 (1:1,000; A19653, ABclonal), anti-phospho-inhibitor of NF-κB (p-IκB)-α (Ser32/36; 1:500; AF2002, Affinity Biosciences, Changzhou, China), anti-IκB-α (1:1,000; AF5002, Affinity), anti-p-IκB kinase (IKK; Ser180/Ser181; 1:500; AF3013, Affinity, China), anti-IKK (1:1,000; AF6014, Affinity) and anti-Histone H3 (1:500; 17168-1-AP, Proteintech, Wuhan, China), and anti-β-actin (1:2,000; 60008-1-Ig, Proteintech) antibodies at 4°C overnight. Membranes were incubated with the secondary antibodies at 37°C for 40 min. The relative intensity of proteins was visualized using electrochemiluminescence reagents (Shanghai 7sea biotech Co., Ltd.) and quantified using Gel-Pro Analyzer 4.0 (Media Cybernetics, Rockville, MD, USA).

Immunofluorescence

Deparaffinized lung tissues were blocked in goat serum (SL038, Solarbio) for 15 min at room temperature. Primary antibodies for S1PR1 (1: 200; Ab11424, Abcam, Cambridge, UK) and F4/80 (1: 50; Sc-377009, Santa Cruz Biotechnology, Dallas, TX, USA) were used to treat tissue samples overnight at 4°C. Tissue samples were stained with corresponding secondary antibodies for 90 min at room temperature. Nuclei were visualized with 4', 6-diamidino-2-phenylindole (DAPI; C1002, Beyotime). After cells were treated with antifade mounting medium, representative images were acquired under fluorescence microscopy (BX53, Olympus) at ×400 magnification.

Dual-luciferase reporter assay

RAW264.7 cells were obtained from Procell Life Science & Technology (Wuhan, China) and cultured in

Dulbecco's Modified Eagle's Medium (12100-46, Gibco, Thermo Fisher Scientific, Waltham, MA, USA) containing 10% fetal bovine serum at 37°C with 5% CO_2. At 70% confluence, cells were seeded in 12-well plates and serum-starved for 1 h. Cells were transfected with a pmirGLO luciferase expression construct containing the wild-type (wt) or mutant (mut) 3'-UTR of *S1pr1*, and miR-363-3p mimic or negative control (NC) mimic using Lipofectamine 3000 (L3000 008, Invitrogen, Thermo Fisher Scientific, Waltham, MA, USA). At 48 h after transfection, luciferase activities were detected using a dual-luciferase reporter assay kit (KGAF040, KeyGEN BioTECH, Nanjing, China) and normalized to Renilla luciferase activity.

Statistical Analysis

Results were expressed as the mean ± SD and analyzed using the GraphPad Prism 8.0 software. Student's *t*-test was used to compare differences between two groups, while one-way ANOVA followed by Tukey's was used for multiple comparisons. For survival analysis, the survival curves were compared using the log-rank test. *P* less than 0.05 was considered statistically significant.

Results

Upregulated miR-363-3p and downregulated S1PR1 were observed in lung tissues of septic mice

As shown in Fig. 1a, the mRNA level of miR-363-3p in the CLP group was remarkably higher than that in the sham group ($P<0.05$), whereas the *S1pr1* level was greatly lower in the CLP group (Fig. 1b, $P<0.05$). The results of the immunofluorescence analysis revealed that the fluorescence intensity of S1PR1 in the CLP group

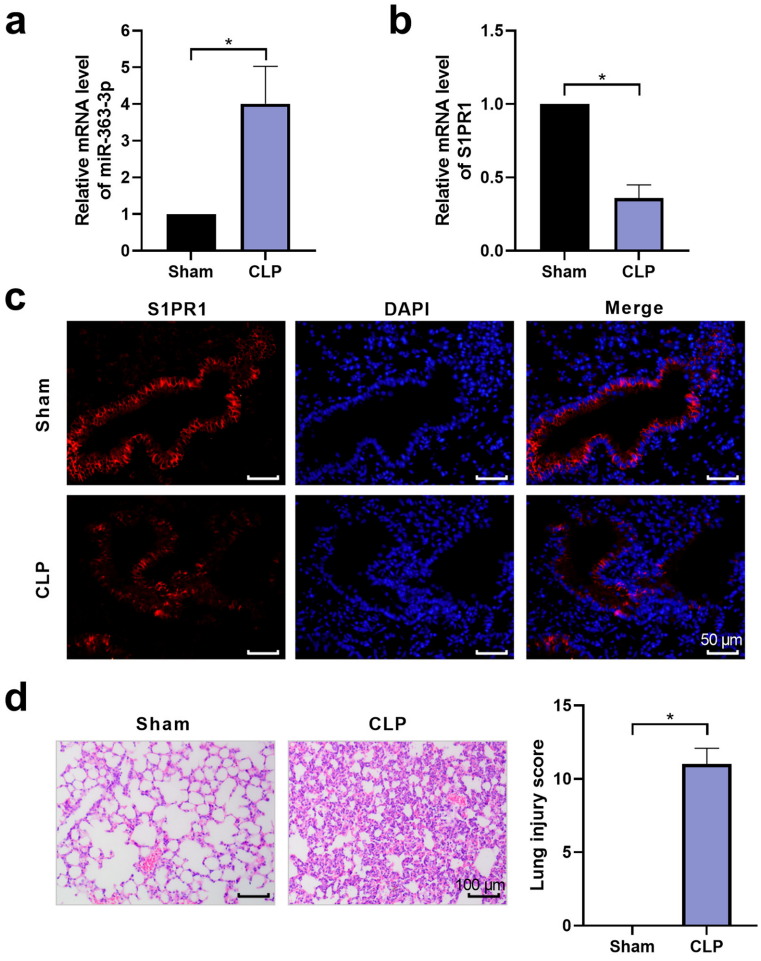

Fig. 1. Upregulation of miR-363-3p and downregulation of S1PR1 are observed in lung tissues of septic mice. (a) Relative mRNA levels of miR-363-3p in lung tissues of mice in different groups. (b) Relative mRNA levels of *S1pr1* in lung tissues of mice in different groups. (c) Representative images of immunofluorescence staining with S1PR1 in lung tissues of mice in different groups. Bars=50 μm. (d) Representative images of H&E staining and pathological scores in lung tissues of mice in different groups. Bars=100 μm. N=6 mice per group. Results are expressed as means ± SD. *$P<0.05$.

was greatly decreased relative to the sham group (Fig. 1c). H&E staining confirmed that there were obvious histopathological injuries in lung tissues of the CLP mice, which exhibited more inflammatory cell infiltration and alveolar structure damage (Fig. 1d, $P<0.05$).

Knockdown of miR-363-3p alleviated pathological injuries in lung tissues of septic mice

To elucidate the effect of miR-363-3p on sepsis-induced ALI, antagomir-363-3p or its control (antagomir NC) was administered to mice by tail vein intravenous injection before the CLP procedure. As shown in Fig. 2a, the injection of antagomir-363-3p into CLP-treated mice significantly decreased the level of miR-363-3p compared with the administration of antagomir NC ($P<0.05$). At the end of the 7 day follow-up period, the survival rate of the sham mice was 100%, while survival rate of the CLP mice decreased significantly to 0% on day 6 after the procedure (Fig. 2b). However, administration of antagomir-363-3p efficiently increased the survival rate after the surgery (Fig. 2b). The results of H&E staining suggested that a majority of the alveolar cavity in the CLP and CLP+antagomir NC groups exhibited exudation, edema, and inflammatory cell infiltration and that the alveolar septal walls were thickened. Importantly, inhibition of miR-363-3p ameliorated CLP-induced lung tissue inflammation, edema, and hemorrhage (Fig. 2c). The pathological scores for lung injury

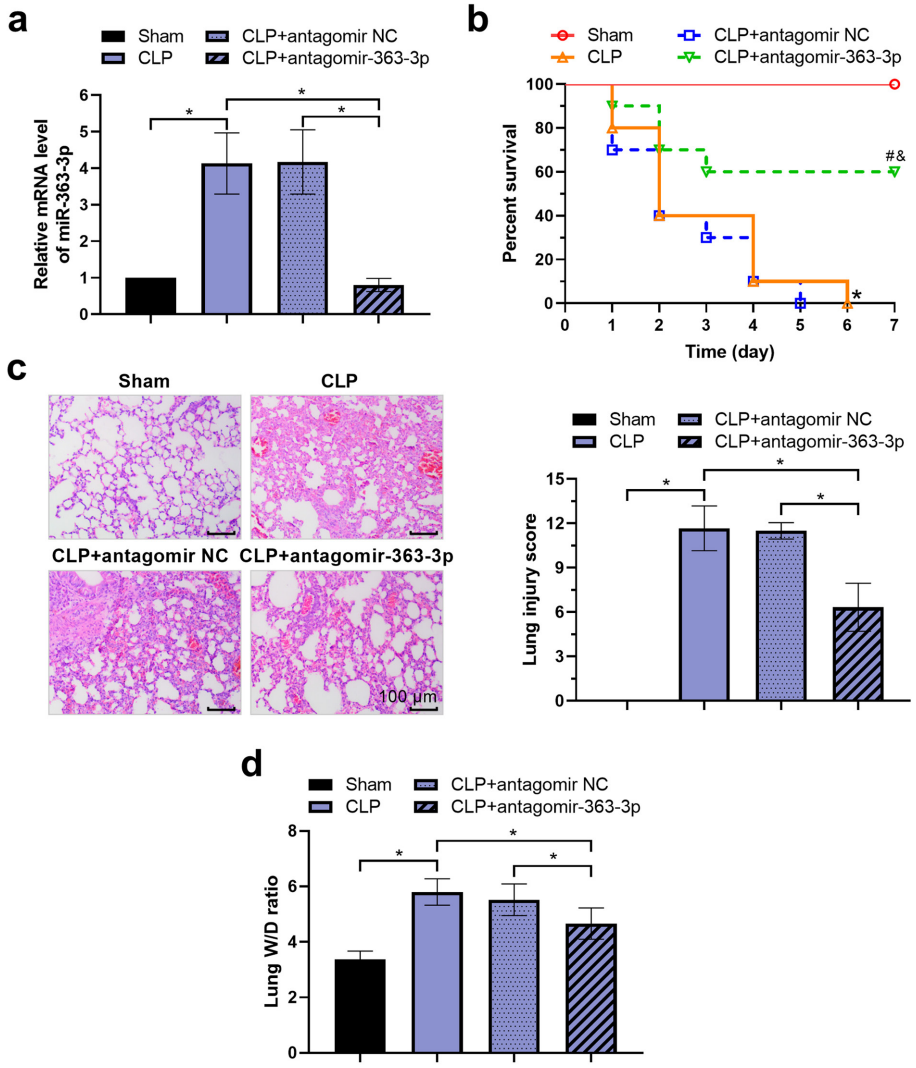

Fig. 2. Knockdown of miR-363-3p alleviates pathological injury in lung tissues of septic mice. (a) Relative mRNA levels of miR-363-3p in lung tissues of mice in different groups. (b) Survival rates of mice within 7 consecutive days following the CLP procedure. (c) Representative images of H&E staining and pathological scores in lung tissues of mice in different groups. Bars=100 μm. (d) The W/D ratios of lung tissues of mice in different groups. N=6 mice per group. Results are expressed as means ± SD. *$P<0.05$, vs. the sham group. $^{\#}P<0.05$, vs. the CLP group. $^{\&}P<0.05$, vs. the CLP+antagomir NC group.

confirmed that the downregulation of miR-363-3p dramatically alleviated pathological damage in lung tissues of mice after the CLP procedure (Fig. 2c, $P<0.05$). Furthermore, knockdown of miR-363-3p dramatically decreased the degree of pulmonary edema in mice after the CLP operation (Fig. 2d, $P<0.05$).

Knockdown of miR-363-3p relieved oxidative stress in lung tissues of septic mice

The effect of miR-363-3p on oxidative stress in lung tissues of septic mice was evaluated. The results suggested that the levels of the antioxidant enzymes SOD and GSH were obviously reduced in the CLP group compared with the sham group, while the ROS and MDA levels were greatly enhanced (Fig. 3a–d, $P<0.05$). Injection of antagomir-363-3p significantly decreased the MDA and ROS levels but increased the activities of the antioxidant enzymes SOD and GSH compared with the CLP+antagomir NC group (Fig. 3a–d, $P<0.05$).

Knockdown of miR-363-3p inhibited the CLP-induced inflammatory response in lung tissues of mice

The effect of miR-363-3p on inflammation was further investigated. The BALF protein concentration in the CLP group was significantly increased compared with that in the sham group, but it was inhibited after knockdown of miR-363-3p (Fig. 4a, $P<0.05$). The results of Wright-Giemsa staining revealed excessive numbers of total cells, macrophages, and neutrophils in the BALF of the CLP group, and these cell numbers were decreased after injection of antagomir-363-3p (Fig. 4b and c, $P<0.05$). Similarly, knockdown of miR-363-3p evidently curbed the CLP-induced increase of lung MPO activity (Fig. 4d, $P<0.05$) as well as the production of the pro-inflammatory cytokines TNF-α and IL-1β (Fig. 4e and f, $P<0.05$).

Knockdown of miR-363-3p decreased CLP-induced PMP formation and TG in mice

We next investigated the role of miR-363-3p on PMP formation and TG in response to CLP. As shown in Fig. 5a and b, CLP increased the levels of PMPs by nearly three-fold compared with the sham operation ($P<0.05$). However, knockdown of miR-363-3p abolished the CLP-induced formation of PMPs. In addition, TG was detected using a commercial kit. The results showed that TG was weakly decreased in plasma harvested from the CLP+antagomir-363-3p groups relative to the CLP and CLP+antagomir NC groups (Fig. 5c).

Knockdown of miR-363-3p blocked the NF-κB activation by targeting S1PR1

A previous study showed that S1PR1 was the target of hsa-miR-363 [19]. To understand the underlying mechanisms of miR-363-3p in CLP-induced septic mice, we further detected the level of S1PR1 by RT-PCR and western blotting. As shown in Fig. 6a and b, knockdown of miR-363-3p markedly upregulated S1PR1 mRNA and

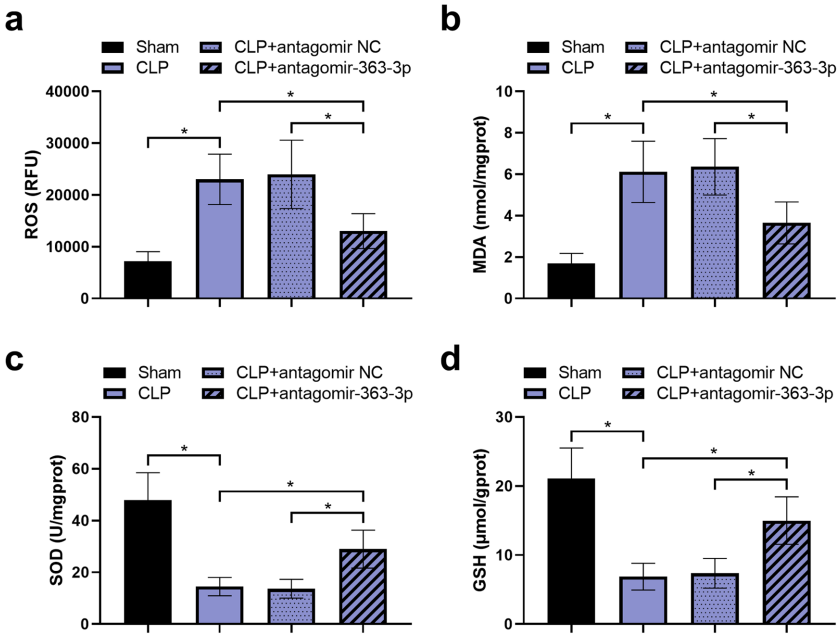

Fig. 3. Downregulation of miR-363-3p relieves oxidative stress in lung tissues of septic mice. (a) ROS fluorescence intensity, (b) MDA content, (c) SOD activity, and (d) GSH activity were detected using commercial kits. N=6 mice per group. Results are expressed as means ± SD. *$P<0.05$.

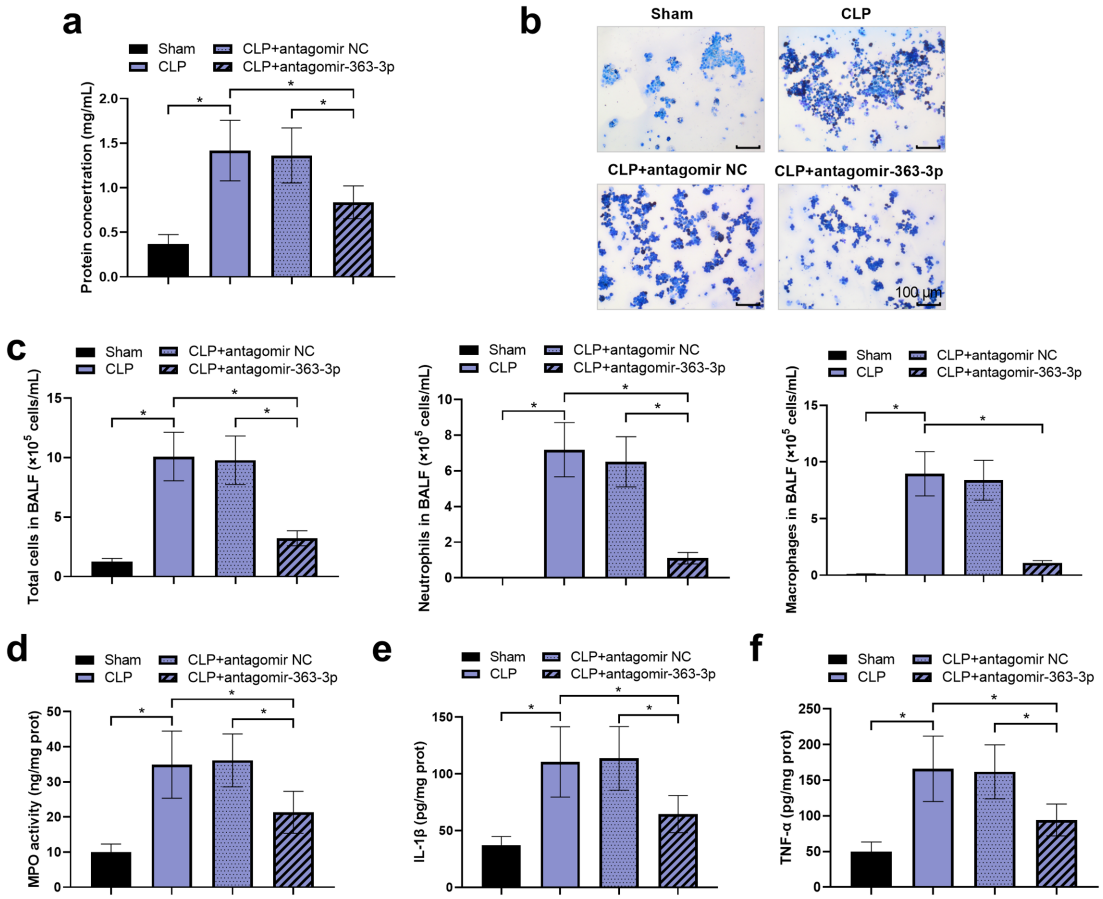

Fig. 4. Knockdown of miR-363-3p inhibits CLP-induced inflammatory responses in lung tissues of mice. (a) BALF protein concentrations in different groups. (b) Representative images of Wright-Giemsa staining in BALF of mice in different groups. (c) The total cell, macrophage, and neutrophil counts in BALF of different groups. (d) Lung MPO activities in different groups. (e) Lung IL-1β levels in different groups. (f) Lung TNF-α levels in different groups. N=6 mice per group. Results are expressed as means ± SD. **P*<0.05.

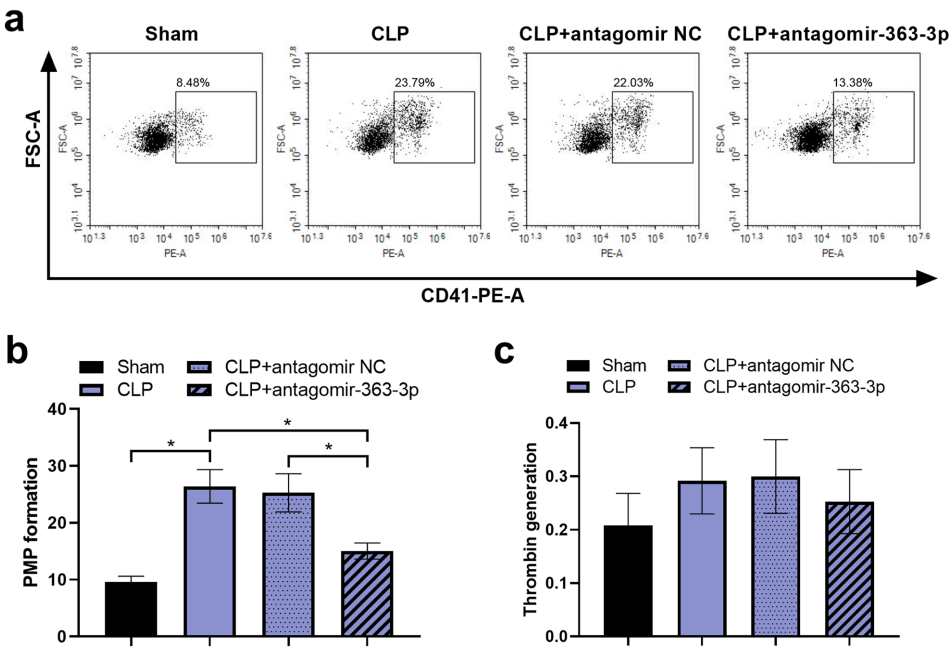

Fig. 5. Knockdown of miR-363-3p decreases CLP-induced PMP formation and TG in mice. (a) Representative dot plots in the blood of different groups by flow cytometry. (b) The numbers of PMPs in the blood of different groups. (c) Levels of total TG in the plasma of different groups. N=6 mice per group. Results are expressed as means ± SD. **P*<0.05.

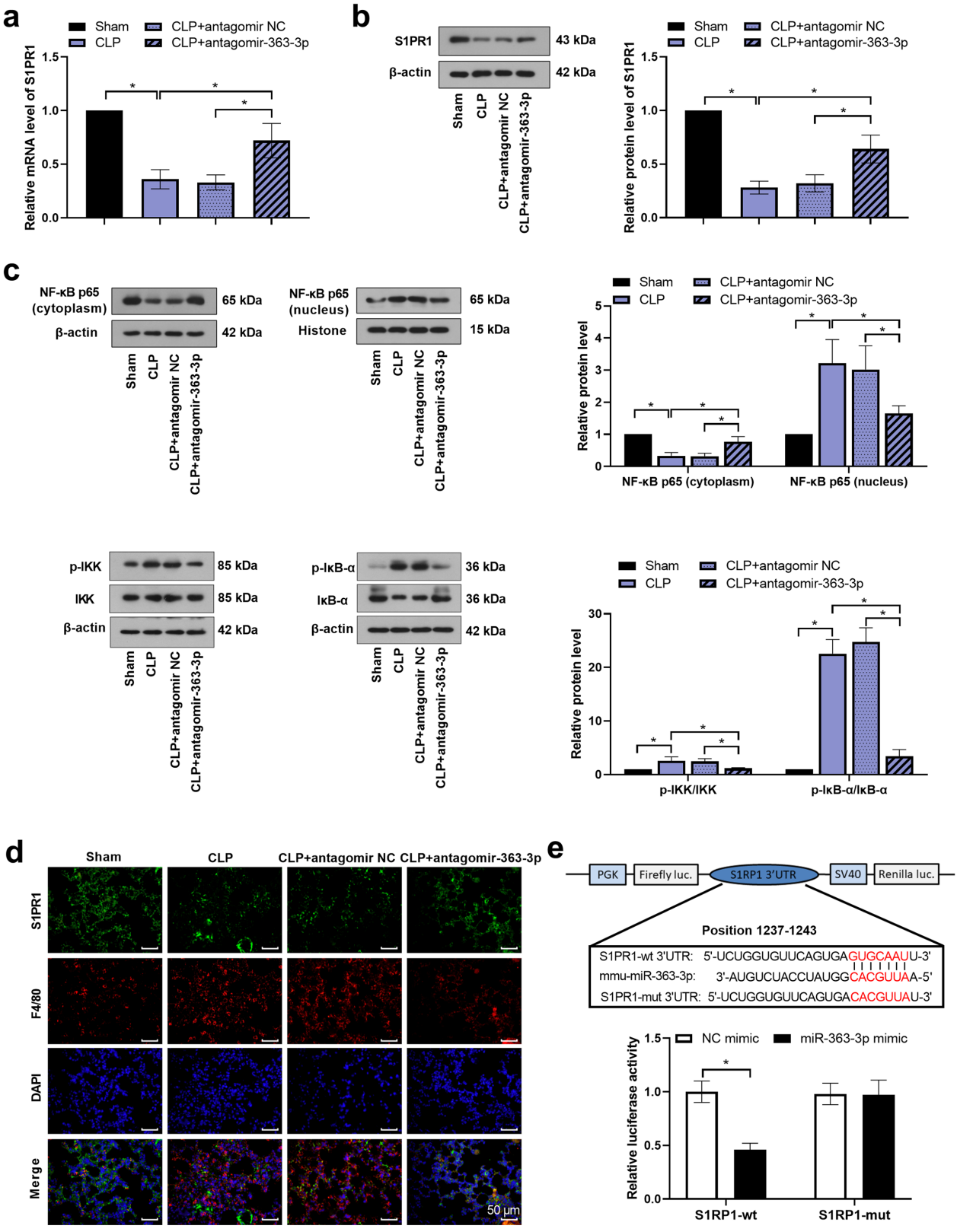

Fig. 6. Knockdown of miR-363-3p blocks the NF-κB activation by targeting S1PR1. (a) Relative mRNA levels of *S1pr1* in lung tissues of mice in different groups. (b) Relative protein levels of S1PR1 in lung tissues of mice in different groups. (c) Relative protein levels of NF-κB p65 (cytoplasm), NF-κB p65 (nucleus), p-IKK $^{Ser180/Ser181}$, IKK, p-IκB-α $^{Ser32/36}$, and IκB-α in lung tissues of mice in different groups. (d) Representative images of dual immunofluorescence staining with S1PR1 and F4/80 in lung tissues of mice in different groups. (e) A luciferase reporter assay was used to measure the relative luciferase activities of S1PR1-3'-UTR wt and mut in RAW264.7 cells. Results were expressed as means ± SD, **P*<0.05.

protein expression in the CLP-induced septic mice (P<0.05). Furthermore, knockdown of miR-363-3p blocked NF-κB p65 translocation from the cytoplasm to the nucleus after the CLP operation (Fig. 6c, P<0.05). Knockdown of miR-363-3p also downregulated the expression of p-IKK/IKK and p-IκB-α/IκB-α (Fig. 6c, P<0.05). The results of dual immunofluorescence suggested that knockdown of miR-363-3p prevented macrophage S1PR1 deletion (Fig. 6d). The TargetScan online database predicted that S1PR1 was a potential target gene of mmu-miR-363-3p (http://www.targetscan.org/vert_72/). The results of the luciferase activity assay revealed that the relative luciferase activity of S1PR1-3'-UTR-wt in RAW264.7 cells in the miR-363-3p mimic group was significantly decreased compared with the NC mimic group (Fig. 6e, P<0.05), but there was no significant difference in the luciferase activity of S1PR1-3'-UTR-mut between the miR-363-3p mimic group and the NC mimic group.

Discussion

Sepsis is a severe infective complication characterized by dysregulated immune responses, vascular occlusion, and subsequent multiple organ failure, and it has become the main etiology of ALI [27]. Despite the implementation of many lung-protective strategies, ALI remains a major clinical problem due to significant morbidity and mortality [28]. Therefore, the discovery of novel therapeutic targets contributes to the management of sepsis-induced ALI. The present study suggested that miR-363-3p was highly expressed in the lung tissues of septic mice. Knockdown of miR-363-3p protected septic mice from ALI by targeting S1PR1, which was implicated in the inactivation of NF-κB signaling. These data highlight the potential therapeutic role of the miR-363-3p/S1PR1/NF-κB axis in septic ALI (Fig. 7).

The essence of ALI is deemed to be an excessive and uncontrolled inflammatory response [29]. Massive lung inflammation destroys the basement membrane and enhances the alveolar-capillary membrane permeability [29]. In this study, we found that CLP induced pulmonary edema, inflammatory cell infiltration, and thickening of alveolar septal walls. CLP also caused the increases in the MPO activity in lung tissues and the inflammatory cell numbers in BALF. The expression of pro-inflammatory cytokines, including TNF-α and IL-1β, was remarkably increased after the CLP operation. However, the above CLP-induced effects were inhibited by miR-363-3p silencing. Furthermore, serious oxidative stress is known to exert a crucial role in the pathogenesis of ALI [30]. ROS generation aggravates lung inflammation, and

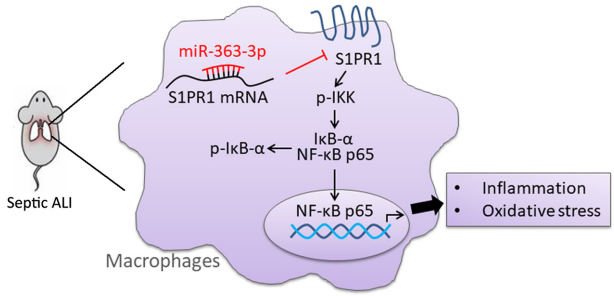

Fig. 7. The functional mechanism of miR-363-3p in septic ALI. The inactivation of NF-κB signaling is implicated in the miR-363-3p/S1PR1 axis-mediated protective effects on septic ALI.

inflammatory cells in turn lead to the overproduction of ROS, which creates a vicious cycle of worsening ALI [30]. A previous study has demonstrated that inhibition of miR-363-3p provides protection against propofol-induced neurotoxicity by inhibiting oxidative stress [10], indicating that miR-363-3p is a key regulator of oxidative stress. In this study, we observed that CLP induced the production of MDA and ROS and inhibited SOD and GSH activities in the lung tissues of mice, which was reversed by miR-363-3p knockdown. Our data demonstrate the anti-inflammatory and antioxidant roles of miR-363-3p suppression in sepsis-induced ALI.

It is well-known that inflammation and coagulation play important roles in the pathogenesis of sepsis and promote each other mutually [31]. Enormous studies have confirmed that the pro-inflammatory factors IL-1β and TNF-α function as mediators of the procoagulant process [32], and contribute to inflammatory responses and tissue injury [33]. As a key factor in sepsis, platelet activation facilitates the neutrophil infiltration in the lung tissues and contributes to blood coagulation via the formation of PMPs [34]. Wang *et al.* found that upregulation of miR-126 markedly inhibited the increased permeability and inflammation induced by thrombin in septic mice [9]. Furthermore, inhibition of Rac1 activity alleviated dysfunctional coagulation in abdominal sepsis via regulation of the formation of PMPs and TG [35]. Here, we determined the role of miR-363-3p in PMP formation and TG in sepsis-induced ALI. Our results revealed that silencing of miR-363-3p decreased the formation of PMPs and TG in septic mice. These findings suggest that inhibition of miR-363-3p could be a useful target to inhibit dysfunctional coagulation in sepsis-induced ALI.

As responsive cells, macrophages play key roles in inflammation and coagulative function during sepsis [36]. A previous study suggested that macrophage S1PR1 deletion enhanced angiogenesis and inflammation in a mouse model of imiquimod-induced psoriasis [15]. An-

other study revealed that platelet aggregation is enhanced by S1PR1 activation [37]. In this study, upregulation of macrophage S1PR1 expression was found in lung tissues of septic mice after miR-363-3p knockdown. Therefore, inflammation and oxidative stress triggered by miR-363-3p upregulation may be associated with a reduced S1PR1 level. The inhibitory effect of miR-363-3p knockdown on coagulation disorders may be caused by regulating other genes. The mechanism related to coagulation disorders caused by miR-363-3p still needs to be further explored. Additionally, NF-κB signaling is an important signaling pathway in tissue inflammatory and immune response, as it transcriptionally modulates the expression of genes [38]. The NF-κB signaling pathway was found to be involved in the ALI mediated by S1PR1 [16]. The selective S1PR1 agonist CYM5442 suppressed innate immune responses in H1N1-infected mice via inactivation of the NF-κB signaling pathways [16]. Here, we assessed the expression of the p65 in the cytoplasm, p65 in the nucleus, IKK, p-IKK, IκB-α, and p-IκB-α, which is necessary for the activation and translocation of NF-κB signaling. IκB-α is destroyed by the IKK, and subsequently, the p65 subunit is released and translocated from the cytoplasm to the nucleus, where it induces downstream inflammatory cytokines [39]. In the current study, activation of IκB/NF-κB signaling was observed in lung tissues of septic mice and blocked after miR-363-3p knockdown. Mechanistically, our study validated *in vivo* that the miR-363-3p/S1PR1 axis might ameliorate sepsis-induced ALI via inactivation of the NF-κB signaling pathway.

In summary, our data elucidate the protective role of miR-363-3p inhibition in lung tissues of septic mice. We determine that knockdown of miR-363-3p alleviates the inflammatory response and oxidative stress by negatively regulating S1PR1, which is associated with the inactivation of NF-κB signaling. Our results show that targeting the miR-363-3p/S1PR1/NF-κB axis may be a useful therapeutic method for sepsis-induced ALI.

Conflict of Interests

The authors declare they have no conflicts of interest.

Acknowledgments

This work was supported by the National Natural Scientific Foundation of China (No. 81772045), the Research and Innovation Fund for Graduate Students of Harbin Medical University (No. yjskycx2018-46hyd) and the Scientific Research Project of Heilongjiang Provincial Health Commission (No. 2019036).

References

1. Schlapbach LJ, Straney L, Bellomo R, MacLaren G, Pilcher D. Prognostic accuracy of age-adapted SOFA, SIRS, PELOD-2, and qSOFA for in-hospital mortality among children with suspected infection admitted to the intensive care unit. Intensive Care Med. 2018; 44: 179–188. [Medline] [CrossRef]
2. Rubenfeld GD, Caldwell E, Peabody E, Weaver J, Martin DP, Neff M, et al. Incidence and outcomes of acute lung injury. N Engl J Med. 2005; 353: 1685–1693. [Medline] [CrossRef]
3. Semeraro N, Ammollo CT, Semeraro F, Colucci M. Sepsis, thrombosis and organ dysfunction. Thromb Res. 2012; 129: 290–295. [Medline] [CrossRef]
4. Zhang H, Mao YF, Zhao Y, Xu DF, Wang Y, Xu CF, et al. Upregulation of Matrix Metalloproteinase-9 Protects against Sepsis-Induced Acute Lung Injury via Promoting the Release of Soluble Receptor for Advanced Glycation End Products. Oxid Med Cell Longev. 2021; 2021: 8889313. [Medline]
5. Kim VN, Han J, Siomi MC. Biogenesis of small RNAs in animals. Nat Rev Mol Cell Biol. 2009; 10: 126–139. [Medline] [CrossRef]
6. Jiang WL, Zhao KC, Yuan W, Zhou F, Song HY, Liu GL, et al. MicroRNA-31-5p exacerbates lipopolysaccharide-induced acute lung injury via inactivating Cab39/AMPKα pathway. Oxid. Med. Cell. Longev. 2020; 2020: 8822361. [Medline] [CrossRef]
7. Wang Y, Wang H, Zhang C, Zhang C, Yang H, Gao R, et al. Plasma Hsa-miR-92a-3p in correlation with lipocalin-2 is associated with sepsis-induced coagulopathy. BMC Infect Dis. 2020; 20: 155. [Medline] [CrossRef]
8. Wang HJ, Deng J, Wang JY, Zhang PJ, Xin Z, Xiao K, et al. Serum miR-122 levels are related to coagulation disorders in sepsis patients. Clin Chem Lab Med. 2014; 52: 927–933. [Medline] [CrossRef]
9. Wang HF, Wang YQ, Dou L, Gao HM, Wang B, Luo N, et al. Influences of up-regulation of miR-126 on septic inflammation and prognosis through AKT/Rac1 signaling pathway. Eur Rev Med Pharmacol Sci. 2019; 23: 2132–2138. [Medline]
10. Yao Y, Zhang JJ. Propofol induces oxidative stress and apoptosis in vitro via regulating miR-363-3p/CREB signalling axis. Cell Biochem Funct. 2020; 38: 1119–1128. [Medline] [CrossRef]
11. Pyne NJ, Tonelli F, Lim KG, Long JS, Edwards J, Pyne S. Sphingosine 1-phosphate signalling in cancer. Biochem Soc Trans. 2012; 40: 94–100. [Medline] [CrossRef]
12. Weigert A, Weis N, Brüne B. Regulation of macrophage function by sphingosine-1-phosphate. Immunobiology. 2009; 214: 748–760. [Medline] [CrossRef]
13. Deng J, Liu Y, Lee H, Herrmann A, Zhang W, Zhang C, et al. S1PR1-STAT3 signaling is crucial for myeloid cell colonization at future metastatic sites. Cancer Cell. 2012; 21: 642–654. [Medline] [CrossRef]
14. Liang J, Nagahashi M, Kim EY, Harikumar KB, Yamada A, Huang WC, et al. Sphingosine-1-phosphate links persistent STAT3 activation, chronic intestinal inflammation, and development of colitis-associated cancer. Cancer Cell. 2013; 23: 107–120. [Medline] [CrossRef]
15. Syed SN, Raue R, Weigert A, von Knethen A, Brüne B. Macrophage S1PR1 Signaling Alters Angiogenesis and Lymphangiogenesis During Skin Inflammation. Cells. 2019; 8: E785. [Medline] [CrossRef]
16. Zhao J, Zhu M, Jiang H, Shen S, Su X, Shi Y. Combination of sphingosine-1-phosphate receptor 1 (S1PR1) agonist and antiviral drug: a potential therapy against pathogenic influenza virus. Sci Rep. 2019; 9: 5272. [Medline] [CrossRef]
17. Feng A, Rice AD, Zhang Y, Kelly GT, Zhou T, Wang T. S1PR1-Associated Molecular Signature Predicts Survival in Patients with Sepsis. Shock. 2020; 53: 284–292. [Medline] [CrossRef]

18. Zhu B, Luo GH, Feng YH, Yu MM, Zhang J, Wei J, et al. Apolipoprotein M Protects Against Lipopolysaccharide-Induced Acute Lung Injury via Sphingosine-1-Phosphate Signaling. Inflammation. 2018; 41: 643–653. [Medline] [CrossRef]
19. Zhou P, Huang G, Zhao Y, Zhong D, Xu Z, Zeng Y, et al. MicroRNA-363-mediated downregulation of S1PR1 suppresses the proliferation of hepatocellular carcinoma cells. Cell Signal. 2014; 26: 1347–1354. [Medline] [CrossRef]
20. Dong J, Geng J, Tan W. MiR-363-3p suppresses tumor growth and metastasis of colorectal cancer via targeting SphK2. Biomed Pharmacother. 2018; 105: 922–931. [Medline] [CrossRef]
21. Jiang J, Huang K, Xu S, Garcia JGN, Wang C, Cai H. Targeting NOX4 alleviates sepsis-induced acute lung injury via attenuation of redox-sensitive activation of CaMKII/ERK1/2/MLCK and endothelial cell barrier dysfunction. Redox Biol. 2020; 36: 101638. [Medline] [CrossRef]
22. McClure C, Ali E, Youssef D, Yao ZQ, McCall CE, El Gazzar M. NFI-A disrupts myeloid cell differentiation and maturation in septic mice. J Leukoc Biol. 2016; 99: 201–211. [Medline] [CrossRef]
23. Li Y, Xia M, Peng L, Liu H, Chen G, Wang C, et al. Downregulation of miR-214-3p attenuates mesangial hypercellularity by targeting PTEN-mediated JNK/c-Jun signaling in IgA nephropathy. Int J Biol Sci. 2021; 17: 3343–3355. [Medline] [CrossRef]
24. Park JK, Kogure T, Nuovo GJ, Jiang J, He L, Kim JH, et al. miR-221 silencing blocks hepatocellular carcinoma and promotes survival. Cancer Res. 2011; 71: 7608–7616. [Medline] [CrossRef]
25. Kral-Pointner JB, Schrottmaier WC, Horvath V, Datler H, Hell L, Ay C, et al. Myeloid but not epithelial tissue factor exerts protective anti-inflammatory effects in acid aspiration-induced acute lung injury. J Thromb Haemost. 2017; 15: 1625–1639. [Medline] [CrossRef]
26. Livak KJ, Schmittgen TD. Analysis of relative gene expression data using real-time quantitative PCR and the 2(-Delta Delta C(T)) Method. Methods. 2001; 25: 402–408. [Medline] [CrossRef]
27. Sagy M, Al-Qaqaa Y, Kim P. Definitions and pathophysiology of sepsis. Curr Probl Pediatr Adolesc Health Care. 2013; 43: 260–263. [Medline] [CrossRef]
28. Bellani G, Laffey JG, Pham T, Fan E, Brochard L, Esteban A, et al. LUNG SAFE Investigators ESICM Trials Group. Epidemiology, Patterns of Care, and Mortality for Patients With Acute Respiratory Distress Syndrome in Intensive Care Units in 50 Countries. JAMA. 2016; 315: 788–800. [Medline] [CrossRef]
29. Williams AE, Chambers RC. The mercurial nature of neutrophils: still an enigma in ARDS? Am J Physiol Lung Cell Mol Physiol. 2014; 306: L217–L230. [Medline] [CrossRef]
30. Karki P, Birukov KG. Rho and Reactive Oxygen Species at Crossroads of Endothelial Permeability and Inflammation. Antioxid Redox Signal. 2019; 31: 1009–1022. [Medline] [CrossRef]
31. Levi M, van der Poll T. Coagulation and sepsis. Thromb Res. 2017; 149: 38–44. [Medline] [CrossRef]
32. Scully M, Levi M. How we manage haemostasis during sepsis. Br J Haematol. 2019; 185: 209–218. [Medline] [CrossRef]
33. Tucker EI, Verbout NG, Leung PY, Hurst S, McCarty OJ, Gailani D, et al. Inhibition of factor XI activation attenuates inflammation and coagulopathy while improving the survival of mouse polymicrobial sepsis. Blood. 2012; 119: 4762–4768. [Medline] [CrossRef]
34. Wang Y, Zhang S, Luo L, Norström E, Braun OO, Mörgelin M, et al. Platelet-derived microparticles regulates thrombin generation via phophatidylserine in abdominal sepsis. J Cell Physiol. 2018; 233: 1051–1060. [Medline] [CrossRef]
35. Wang Y, Luo L, Mörgelin M, Thorlacius H. Rac1 regulates sepsis-induced formation of platelet-derived microparticles and thrombin generation. Biochem Biophys Res Commun. 2017; 487: 887–891. [Medline] [CrossRef]
36. Moussa MD, Santonocito C, Fagnoul D, Donadello K, Pradier O, Gaussem P, et al. Evaluation of endothelial damage in sepsis-related ARDS using circulating endothelial cells. Intensive Care Med. 2015; 41: 231–238. [Medline] [CrossRef]
37. Liu H, Jackson ML, Goudswaard LJ, Moore SF, Hutchinson JL, Hers I. Sphingosine-1-phosphate modulates PAR1-mediated human platelet activation in a concentration-dependent biphasic manner. Sci Rep. 2021; 11: 15308. [Medline] [CrossRef]
38. Afonina IS, Zhong Z, Karin M, Beyaert R. Limiting inflammation-the negative regulation of NF-κB and the NLRP3 inflammasome. Nat Immunol. 2017; 18: 861–869. [Medline] [CrossRef]
39. Mulero MC, Huxford T, Ghosh G. NF-κB, IκB, and IKK: Integral Components of Immune System Signaling. Adv Exp Med Biol. 2019; 1172: 207–226. [Medline] [CrossRef]